

# BNAS-v2: Memory-efficient and Performance-collapse-prevented Broad Neural Architecture Search

Zixiang Ding, *Member, IEEE*, Yaran Chen, *Member, IEEE*, Nannan Li and Dongbin Zhao, *Fellow, IEEE*

**Abstract**—Benefit from Broad Convolutional Neural Network (BCNN), Broad Neural Architecture Search (BNAS) achieves state-of-the-art efficiency in reinforcement learning-based NAS approaches. Particularly, BCNN has two novel characteristics, fast single-step training speed and efficient memory (i.e. larger batch size for architecture search), that all contribute to improve the efficiency of NAS. However, only the former advantage plays an important role in BNAS, due to the latter one makes the unfair training issue worse.

In this paper, we propose BNAS-v2 to further improve the efficiency of NAS, embodying both superiorities of BCNN simultaneously. To mitigate the unfair training issue in BNAS, we employ continuous relaxation strategy to make each edge of cell in BCNN relevant to all candidate operations, so that the gradient-based optimization algorithm of BNAS-v2 can update every possible path simultaneously rather than the single sampled one in BNAS. Moreover, the continuous relaxation strategy relaxes the choice of a candidate operation as a softmax over all predefined operations. However, continuous relaxation leads to another issue named performance collapse, where those weight-free operations are prone to be selected by the search strategy. For this consequent issue, two solutions are given: 1) we propose Confident Learning Rate (CLR) that considers the confidence of gradient for architecture weights update, increasing with the training time of over-parameterized BCNN; 2) we introduce the combination of partial channel connections and edge normalization that also can improve the memory efficiency further. Moreover, we denote differentiable BNAS (i.e. BNAS with continuous relaxation) as BNAS-D, BNAS-D with CLR as BNAS-v2-CLR, and partial-connected BNAS-D as BNAS-v2-PC. Experimental results on CIFAR-10 and ImageNet show that 1) BNAS-v2 delivers state-of-the-art search efficiency on both CIFAR-10 (0.05 GPU days that is 4x faster than BNAS) and ImageNet (0.19 GPU days); and 2) the proposed CLR is effective to alleviate the performance collapse issue in both BNAS-D and vanilla differentiable NAS framework.

## I. INTRODUCTION

NAS has achieved unprecedented accomplishments in the field of structure design engineering. However, it needs enormous computational requirements, e.g. 22400 GPU days for vanilla NAS [1]. The time consuming issue is mitigated by cell, a micro search space proposed in NASNet [2]. Currently, most of NAS approaches [3, 4, 5, 6, 7, 8, 9] are cell-based, where two types of cells (i.e. normal and reduction

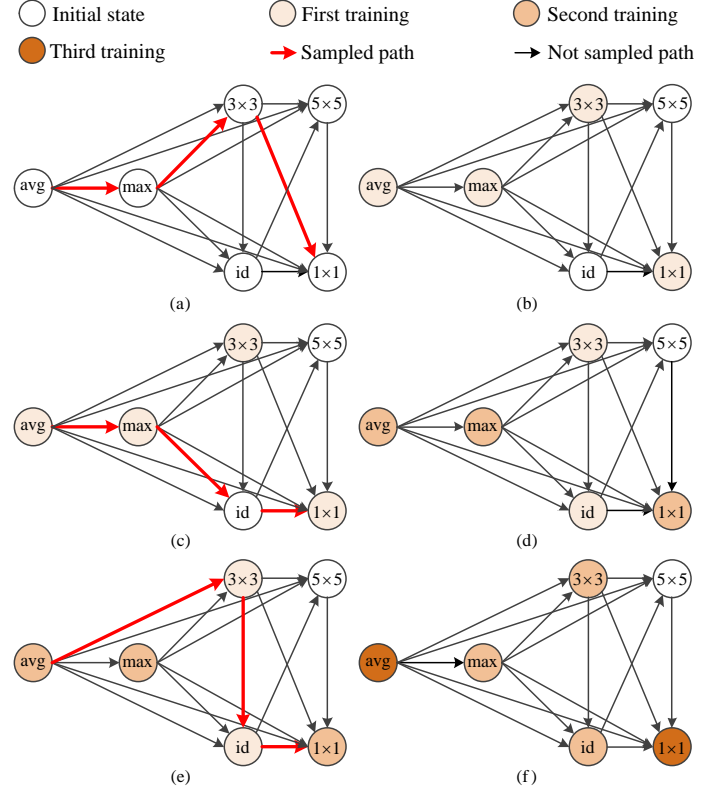


Fig. 1. Unfair training issue in BNAS. A cell can be treated as a path of directed acyclic graph (DAG). (a) BNAS employs a controller to sample a path (red line) from the DAG with a policy  $\pi(\cdot)$ ; (b) Those operations on the sampled path are trained with a mini-batch training data; (c) The controller samples another path with policy  $\pi(\cdot)$ ; (d) Those operations on the sampled path inherit the weights of previous training step, and are trained with another mini-batch training data; (e) Repeat the above sampling step; (f) Repeat the corresponding training step until an epoch is over. Subsequently, the policy  $\pi(\cdot)$  is updated by policy gradient-based RL algorithm that prefers those well trained operations (e.g.  $1 \times 1$  convolution in (f)) rather than not trained well ones (e.g.  $5 \times 5$  convolution in (f)), due to the former one can obtain higher validation accuracy, i.e. reward. However, if the DAG is trained complete, the convolution with  $5 \times 5$  kernel size has larger possibility to obtain higher performance than  $1 \times 1$  convolution. Best viewed in color.

cells) are treated as the building blocks of a deep scalable architecture. However, the above deep scalable architecture is time-consuming for both phases of architecture search and evaluation, due to slow single-step training speed and inefficient memory when using multiple cells.

To solve the above issue, Ding et al. [10] proposed BNAS where a broad network paradigm dubbed BCNN was em-

Z. Ding, Y. Chen, N. Li and D. Zhao are with the State Key Laboratory of Management and Control for Complex Systems, Institute of Automation, Chinese Academy of Sciences, Beijing 100190, China, and also with the University of Chinese Academy of Sciences, Beijing 100049, China (email : {dingzixiang2018, chenyan2013, linannan2017, dongbin.zhao}@ia.ac.cn).

This work is supported partly by the National Natural Science Foundation of China (NSFC) under Grants No. 62006226.

played as the scalable architecture. Different from previous deep scalable architecture, BCNN could use few cells to deliver competitive performance with broad topology. There were two merits of broad topology compared with the deep one, 1) faster single-step training speed and 2) higher memory efficiency (i.e. architecture search with more training data in a mini-batch), that all conducive to the efficiency improvement of NAS. BNAS delivered state-of-the-art search efficiency of 0.20 GPU days with the combination of Reinforcement Learning (RL) [11] and parameters sharing [3]. However, the above optimization strategy of BNAS suffered from the unfair training issue [12] depicted in Fig. 1. On one hand, the above issue led to the learned architecture with poor performance. On the other hand, the second virtue of BCNN potentially made the above issue worse, due to larger batch size (i.e. higher memory efficiency) would reduce the sample times in a single epoch. As a result, only the virtue of fast single-step training speed of BCNN worked for efficiency improvement of BNAS.

In this paper, we propose memory-efficient and performance-collapse-prevented BNAS named BNAS-v2. Particularly, to mitigate the unfair training issue in BNAS, we employ continuous relaxation strategy to make each edge of cell in BCNN relevant to all candidate operations. Moreover, the continuous relaxation strategy relaxes the choice of a candidate operation as a softmax over all predefined operations. As a result, gradient-based optimization algorithm can be employed to simultaneously update total over-parameterized BCNN in BNAS-v2, instead of the single sampled path in BNAS. Furthermore, BNAS-v2 benefits from the memory efficiency of BCNN that contributes to the efficiency improvement and uncertainty reduction for architecture search simultaneously [8]. However, performance collapse issue [7] where those weight-free operations are prone to be selected by the search strategy, arises in differentiable BNAS denoted as BNAS-D, resulting in poor performance of architecture learned by BNAS-D. To mitigate the consequent issue, we give two solutions for BNAS-D. On one hand, we propose Confident Learning Rate (CLR) that considers the confidence of gradient for architecture weights update, increasing with the training time of over-parameterized BCNN. On the other hand, we introduce the combination of partial channel connections and edge normalization [8] that also can further improve the memory efficiency for BNAS-D. Moreover, we denote BNAS-D with CLR as BNAS-v2-CLR, and another partial-connected one as BNAS-v2-PC. Experimental results on CIFAR-10 and ImageNet show that 1) BNAS-v2-CLR and BNAS-v2-PC achieve 2.22x (0.09 GPU days) and 4x (state-of-the-art efficiency of 0.05 GPU days) faster search speed than BNAS on CIFAR-10, respectively; 2) BNAS-v2-PC can directly search on ImageNet with state-of-the-art efficiency of 0.19 GPU days; 3) compared with BNAS, the architectures learned by BNAS-v2 also deliver better performance on CIFAR-10, and competitive performance on ImageNet; and 4) the proposed CLR is not only effective to mitigate the performance collapse issue in BNAS-D, but also vanilla differentiable NAS pipeline [4].

The remainder of this paper is organized as follows. We

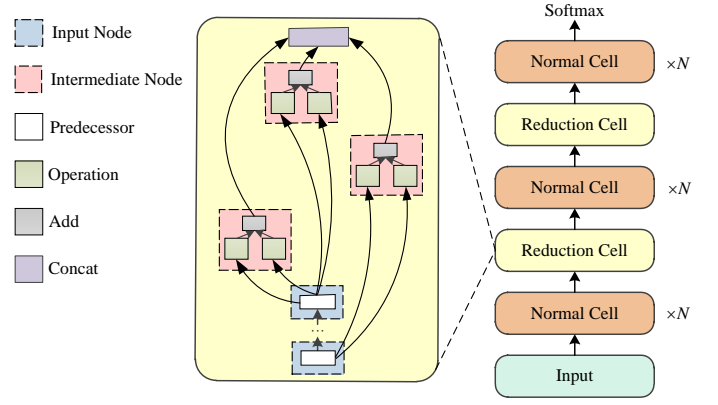


Fig. 2. Deep scalable architecture. Best viewed in color.

review related work in Section II, and introduce the proposed approach in Section III. Subsequently, Section IV shows experiments and corresponding result analysis. At last, we conclude in Section V.

## II. RELATED WORK

Hand-crafted neural networks (e.g. ResNet [13], GoogleNet [14]) played a predominant role in solving computer vision [15, 16, 17, 18, 19, 20], natural language processing [21] and other artificial intelligence related tasks [22, 23, 24, 25] before NAS [1] was proposed. Recent years, NAS achieved unprecedented success in various tasks, e.g. image classification [2, 3, 4, 26, 27], semantic segmentation [28], federated learning [29].

Vanilla NAS [1] greatly suffered from the issue of time consuming. NASNet [2] was proposed to address the above issue, where a micro search space named cell was used to reduce the computational requirements in architecture search phase. Moreover, two types of cells were stacked one after another as a deep scalable architecture shown in Fig. 2. Subsequently, lots of cell-based NAS approaches were proposed to further improve the efficiency of NAS, e.g. evolutionary algorithm-based LEMONADE [30], RL-based ENAS [3], gradient-based DARTS [4] and a series of variants of DARTS (e.g. SNAS [6], P-DARTS [5], PC-DARTS [8]). DARTS transferred the NAS problem from discrete space to continuous one, and employed gradient-based algorithm to optimize the architecture weights. Furthermore, PC-DARTS adopted the combination of partial channel connections and edge normalization to realize memory-efficient DARTS with efficiency improvement.

Beyond that, a broad scalable architecture dubbed BCNN was proposed in RL-based BNAS [10]. Inspired by Broad Learning System (BLS) [31], BCNN employed broad (i.e. shallow) topology to obtain faster single-step training speed and higher memory efficiency than the deep one [2]. Moreover, two variants named BNAS-CCE and BNAS-CCLE with different broad topology were also proposed for performance promotion. Compared with ENAS [3], BNAS delivered 2.25x less computation cost, 0.2 GPU day that ranked the best in RL-based NAS pipelines. However, only the advantage of fast single-step training speed contributed to the efficiency

TABLE I  
PERFORMANCE COMPARISON OF BNAS AND ITS TWO VARIANTS ON  
CIFAR-10 [10].

Architecture	Search Cost <sup>†</sup> (GPU days)	Test Error (%) <sup>‡</sup>		
		Small	Medium	Large
BNAS	0.20	3.83	3.46	2.97
BNAS-CCLE	0.20	3.63	3.40	2.95
BNAS-CCE	<b>0.19</b>	<b>3.58</b>	<b>3.24</b>	<b>2.88</b>

<sup>†</sup> Searched on a single NVIDIA GTX 1080Ti GPU.

<sup>‡</sup> Each group of cells learned by BNAS or its two variants is stacked to small (about 0.5 millions), medium (about 1.1 millions) and large-size (about 4 millions) models.

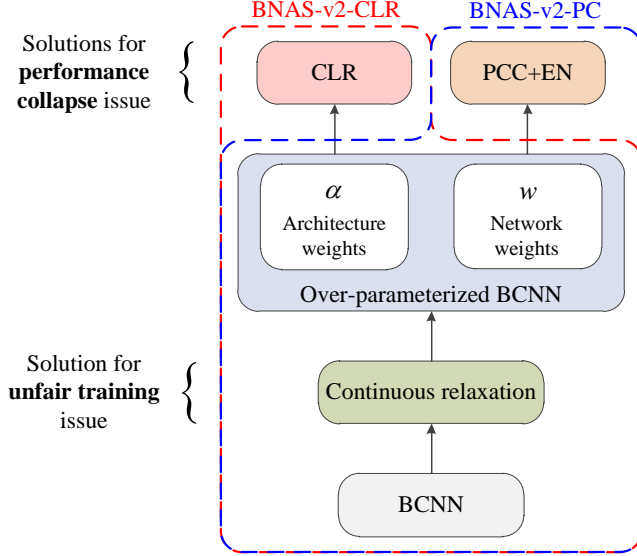


Fig. 3. Overview of BNAS-v2. Continuous relaxation is employed to mitigate the aforementioned unfair training issue, so as to BNAS-2 can take full advantages of BCNN, i.e. fast single-step training speed and efficient memory. Consequently, performance collapse issue arises. For the consequent issue, we propose CLR and introduce the combination of partial channel connections (PCC) and edge normalization (EN). Moreover, the later one is able to improve the memory efficiency of BNAS-v2 further so that BNAS-v2-PC can directly discover architecture on ImageNet. Best viewed in color.

improvement of BNAS, due to high memory efficiency (i.e. large batch size) aggravated the unfair training issue of over-parameterized BCNN.

### III. MEMORY-EFFICIENT AND PERFORMANCE-COLLAPSE-PREVENTED BNAS

As aforementioned, there are three types of BCNNs in BNAS with different performances shown in TABLE I [10]. Obviously, BNAS-CCE delivers the best performance with respect to both efficiency and accuracy. As a result, we treat the BCNN employed in BNAS-CCE as the broad scalable architecture for BNAS-v2.

The overview of BNAS-v2 is shown in Fig. 3. To mitigate the unfair training issue, we employ continuous relaxation for the fairness of over-parameterized BCNN. Furthermore, two solutions are given to mitigate the consequent issue of continuous relaxation, i.e. performance collapse. On one hand, we propose Confident Learning Rate (CLR) that considers the confidence of gradient for architecture weights update

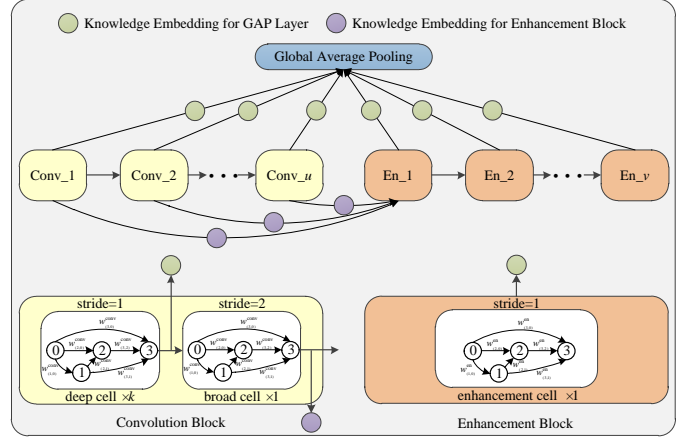


Fig. 4. Broad Convolutional Neural Network. There are four components: *convolution block* for feature extraction, *enhancement block* for feature enhancement, *knowledge embedding* for feature significance control and *multi-scale feature fusion* for the guarantee of high-performance BCNN. Best viewed in color.

increasing with the training time of over-parameterized BCNN. On the other hand, we introduce the combination of partial channel connections and edge normalization [8] that also can improve the memory efficiency further, so that BNAS-v2-PC can directly discover architecture on ImageNet.

#### A. Preliminaries: Broad Convolutional Neural Network

We show the structure of cell-based BCNN in Fig. 4. There are four components: *convolution block*, *enhancement block*, *knowledge embedding* and *multi-scale feature fusion*. *Convolution block* employs  $k$  deep cells (stride=1) and a single broad cell (stride=2) for deep and broad feature extraction, respectively. The first *enhancement block* treats the outputs of every broad cell as input for representation enhancement. All *enhancement blocks* (stride=1) are stacked one after another. *Knowledge embedding* is inserted into BCNN to control the significance of the output of each *convolution block* for the Global Average Pooling (GAP) layer and the first *enhancement block*. *Multi-scale feature fusion* realizes that the GAP can fuse multi-scale feature to more comprehensive representation for high classification accuracy with broad (i.e. shallow) topology.

#### B. Continuous Relaxation of BCNN for Unfair Training

Each cell in BCNN (i.e. deep, broad or enhancement cell) is a directed acyclic graph containing  $N$  nodes: 2 input nodes  $\{x_{(0)}, x_{(1)}\}$ ,  $N-3$  intermediate nodes  $\{x_{(2)}, \dots, x_{(N-2)}\}$ , and a single output node  $x_{(N-1)}$ . Each intermediate node  $x_{(i)}$  is a set of feature maps obtained by operations  $o_{(i,j)}(\cdot)$ , which are chosen from a predefined search space  $\mathcal{O}$  consisting of multiple candidate operations (e.g. convolution, pooling) and used to transform  $x_{(j)}$ . Hence, each intermediate node can be represented by

$$x_{(i)} = \sum_{j < i} o_{(i,j)}(x_{(j)}). \quad (1)$$

The output of cell is obtained by concatenating the outputs of all intermediate nodes.

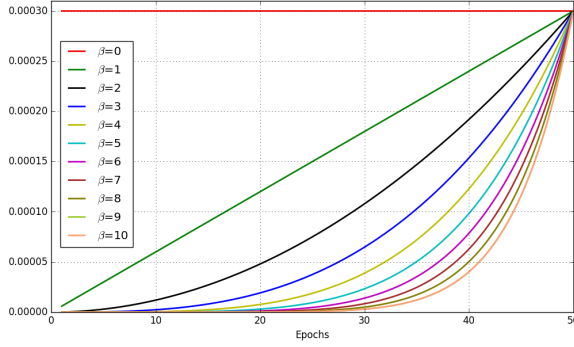


Fig. 5. The curves of CLR under various confidence factors with default architecture learning rate 0.0003 for differentiable NAS approaches. Best viewed in color.

In order to alleviate the unfair training issue, we make each intermediate node relevant to all candidate operations where the output of all predecessor nodes are treated as input, so that the optimization algorithm of BNAS-v2 can update every possible path (i.e. cell) simultaneously rather than the single sampled one in BNAS. Inspired by the strategy of continuous relaxation [4], we relax edge  $(i, j)$  of each cell for over-parameterized BCNN by

$$f_{(i,j)}(x_{(j)}) = \sum_{o \in \mathcal{O}} \frac{\exp(\alpha_{(i,j)}^o)}{\sum_{o' \in \mathcal{O}} \exp(\alpha_{(i,j)}^{o'})} o(x_{(j)}), \quad (2)$$

where, operation  $o(x_{(j)})$  is weighted by a hyper-parameter  $\alpha_{(i,j)}^o$  of dimension  $|\mathcal{O}|$ . Subsequently, BNAS is developed to differentiable BNAS denoted as BNAS-D so that gradient-based algorithm can be employed for parameter optimization. In this paper, we denote  $\alpha$  as architecture weights, and the parameters of operations  $w$  as network weights.

### C. Two Solutions to Prevent Performance Collapse

After continuous relaxation, BNAS-D is able to take two advantages of BCNN, so that it is memory-efficient. However, a consequent issue of continuous relaxation arises that leads to poor performance of BCNN learned by BNAS-D. The above issue is denoted as performance collapse [7] where optimization algorithm prefers to choose those weight-free operations, e.g. skip connection, pooling. To mitigate this consequent issue, two solutions are provided and shown as below.

1) *Confident Learning Rate*: Compared with those weight-equipped operations (e.g. convolution), weight-free operations tend to obtain larger weights before the weights of over-parameterized BCNN are well optimized [8]. In other words, the confidence of gradient obtained from over-parameterized BCNN should increase with the training time for architecture weights update, so that CLR with respect to the number of current epoch is proposed as

$$lr_{conf}(t) = \left(\frac{t}{T}\right)^\beta \times lr_\alpha, \quad (3)$$

where,  $t$  denotes the current epoch from 1 to the maximum  $T$ ,  $\beta$  represents the confidence factor whose value is directly proportional to the confidence of early over-parameterized

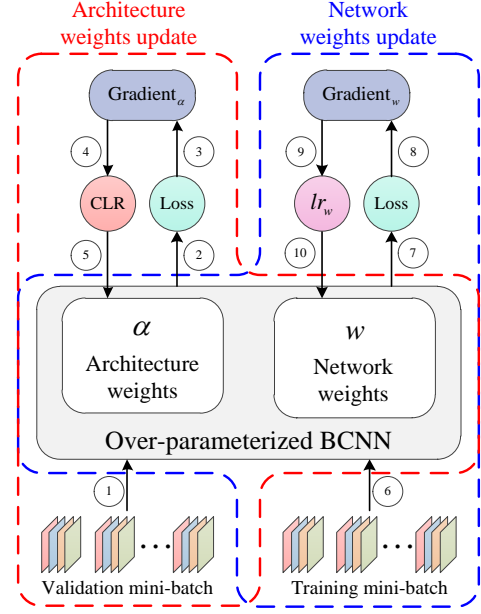


Fig. 6. Overview for BNAS-v2-CLR optimization. For architecture search, there is a loop as below. 1) *Architecture weights update*: ① An validation mini-batch is fed into the broad scalable architecture, to ② obtain the loss for ③ computing the gradient with respect to architecture weights. The proposed CLR is applied for ④ building confident gradient, i.e.  $grad_{conf} = lr_{conf} * \nabla_{\alpha} \mathcal{L}_{val}(w - \xi \nabla_w \mathcal{L}_{train}(w, \alpha), \alpha)$ , for ⑤ architecture weights update. 2) *Network weights update*: ⑥ A training mini-batch is treated as the input of broad scalable architecture. Subsequently, ⑦ the loss is obtained and ⑧ the gradient with regard to network weights is computed. Finally, ⑨ the product of learning rate  $lr_w$  and gradient with respect to  $w$ , i.e.  $lr_w * \nabla_w \mathcal{L}_{train}(w, \alpha)$  is employed for ⑩ network weights update. Best viewed in color.

BCNN, and  $lr_\alpha$  is the initial learning rate for architecture weights. For intuitive comprehension, we plot the curves of CLR under different confidence factors in Fig. 5 where  $lr_\alpha = 0.0003$  is the default setting for differentiable NAS framework [4].

How to determine the value of confidence factor  $\beta$  is an intractable problem. With  $\beta$  increasing, more epochs of early training process are involved to freeze the architecture weights, similar to the strategy of warmup used in PC-DARTS (i.e. training architecture weights after 15 epochs). We make a criterion for  $\beta$  determination as follows.

**Criterion 1:** *The optimal confidence factor should make the architecture weights start to be updated at about 15-th epoch for BNAS-v2.*

2) *Partial Channel Connections and Edge Normalization*: For the connection from  $x_{(j)}$  to  $x_{(i)}$ , partial channel connections (PCC) [8] feeds partial channels into  $|\mathcal{O}|$  operations, and copies others to the output directly. Consequently, the continuous relaxation of BNAS-v2-PC can be computed by

$$f_{(i,j)}^{PC}(x_{(j)}; M_{(i,j)}) = \sum_{o \in \mathcal{O}} \frac{\exp(\alpha_{(i,j)}^o)}{\sum_{o' \in \mathcal{O}} \exp(\alpha_{(i,j)}^{o'})} o(M_{(i,j)} * x_{(j)}) + (1 - M_{(i,j)}) * x_{(j)}, \quad (4)$$

where,  $M_{(i,j)}$  denotes channels sampling mask whose values are chosen from 0 (masked channels) and 1 (selected channels),  $M_{(i,j)} * x_{(j)}$  represents the chosen channels and



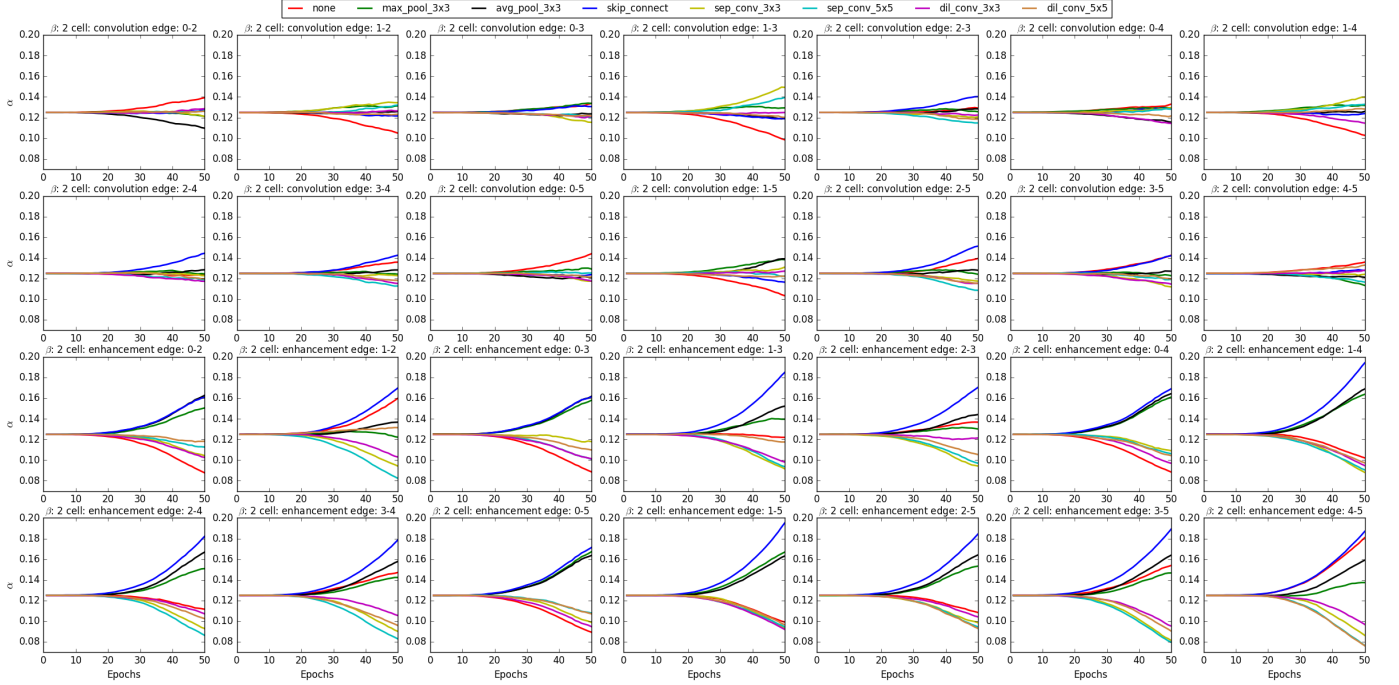


Fig. 7. Performance collapse issue of convolution (subgraph 1 to 14) and enhancement (subgraph 15 to 28) cells in BNAS-v2-CLR ( $\beta = 2$ ) with *skip connection*. Almost all edges choose *skip connection* as operations in enhancement cell that leads to poor-performance BCNN. Best viewed in color.

$(1 - M_{(i,j)}) * x_{(j)}$  computes the masked one. Benefit from PCC, the memory usage of BNAS-v2-PC is reduced greatly, so that larger batch size can be set and higher efficiency can be achieved compared with BNAS-v2-CLR.

After the strategy of PCC, only small part of input channels are fed into the operation mixture that alleviates performance collapse issue [8]. However, PCC also causes undesired fluctuation in the architecture learning process. To mitigate the above problem, we employ edge normalization where edge  $(i, j)$  is weighted by another hyper-parameter denoted as  $\gamma_{(i,j)}$ , so that  $x_{(i)}$  can be computed as

$$x_{(i)}^{PC} = \sum_{j < i} \frac{\exp(\gamma_{(i,j)})}{\sum_{j' < i} \exp(\gamma_{(i,j')})} \cdot f_{(i,j)}(x_{(j)}). \quad (5)$$

The operation  $o_{(i,j)}$  of final architecture is determined by

$$o_{(i,j)} = \operatorname{argmax}_{o \in \mathcal{O}} \frac{\exp(\alpha_{(i,j)}^o)}{\sum_{o' \in \mathcal{O}} \exp(\alpha_{(i,j)}^{o'})} \cdot \frac{\exp(\gamma_{(i,j)})}{\sum_{j' < i} \exp(\gamma_{(i,j')})}. \quad (6)$$

#### D. Optimization Strategies for BNAS-v2

Benefit from continuous relaxation, gradient-based algorithm can be employed for architecture optimization. We propose different strategies to optimize BNAS-v2-CLR and BNAS-v2-PC, due to various solutions for performance collapse.

1) *Architecture Search for BNAS-v2-CLR*: We show the training process in Fig. 6. Similar to vanilla differentiable NAS pipeline [4], BNAS-v2-CLR updates  $\alpha$  and  $w$  by descending  $\nabla_w \mathcal{L}_{train}(w, \alpha)$  and  $lr_{conf} * \nabla_{\alpha} \mathcal{L}_{val}(w - \xi \nabla_w \mathcal{L}_{train}(w, \alpha), \alpha)$ , respectively. Moreover,  $\xi$  is used to

#### Algorithm 1: Architecture Search for BNAS-v2-PC

- 1 For each edge  $(i, j)$ , use (4) and (5) for continuous relation as  $f_{(i,j)}^{PC}(x_{(j)}^{PC}; M_{(i,j)})$  parameterized by  $\alpha_{(i,j)}$  and  $\gamma_{(i,j)}$ ;
- 2 **while not converged do**
- 3     Optimize  $w$  by descending  $\nabla_w \mathcal{L}_{train}(w, \alpha, \gamma)$ ;
- 4     Optimize  $\alpha$  and  $\gamma$  by descending  $\nabla_{\alpha} \mathcal{L}_{val}(w - \xi \nabla_w \mathcal{L}_{train}(w, \alpha, \gamma), \alpha, \gamma)$ ;
- 5 **end**
- 6 Determine  $o_{(i,j)}$  by (6).

control the approximation order (i.e.  $\xi = 0$  is 1st order and  $\xi > 0$  is 2nd order), and  $\mathcal{L}$  represents loss function.

2) *Architecture Search for BNAS-v2-PC*: The proposed architecture optimization algorithm is shown in **Algorithm 1**. There are several differences between the optimization strategies of BNAS-v2-CLR and BNAS-v2-PC as follows.

- BNAS-v2-PC employs the strategy of PCC and EN to construct partial-connected over-parameterized BCNN;
- The architecture learned by BNAS-v2-PC is not only determined by  $\alpha$  but also  $\gamma$ .

## IV. EXPERIMENTS

### A. Datasets and Implementation Details

1) *Datasets*: Similar to previous works [2, 5, 6], CIFAR-10 [32] and ImageNet [33] are also selected for BNAS-v2. There are 60K images with spatial resolution of  $32 \times 32$  in CIFAR-10 [32], where 50K for training and 10K for test. A list of standard methods are applied for preprocessing of CIFAR-10, e.g. randomly flipping and cropping. ImageNet [33] is

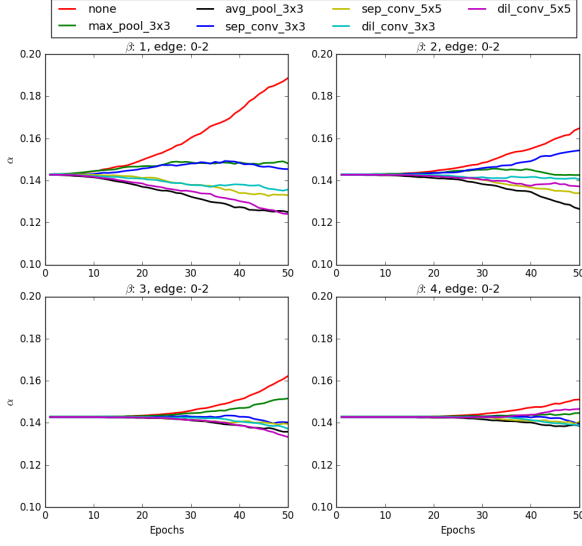


Fig. 8. The architecture weights of each operation on the shallowest edge for BNAS-v2-CLR under various confidence factors. Best viewed in color.

a popular dataset for large scale image classification task. There are about 1.3M images with various spatial resolutions in ImageNet, that are near equally distributed over 1000 object categories. Similarly, a series of data preprocessing techniques are applied to ImageNet. Following previous works [2, 4, 5, 6, 7, 8], we reshape the size of original images of ImageNet to  $224 \times 224$ .

2) *Implementation Details*: BNAS-v2-CLR uses CIFAR-10 for architecture search and ImageNet for transferability verification. Differently, we do not only employ BNAS-v2-PC to directly search on CIFAR-10 but also ImageNet. In previous works [4, 8], search space  $\mathcal{O}$  consists of 8 operations, i.e. *separable convolution* with  $3 \times 3$  and  $5 \times 5$  kernels, *dilated separable convolution* with  $3 \times 3$  and  $5 \times 5$  kernels, *max pooling* and *average pooling* with  $3 \times 3$  kernel, *skip connection*, and *zero (none)*. We still utilize the above candidate operations as search space for BNAS-v2-PC. Differently, *skip connection* is removed for the search space of BNAS-v2-CLR, due to CLR can alleviate the collapse issue in convolution cell rather than enhancement cell. In the architecture search phase of BNAS-v2-CLR, *skip connection* is predominant for almost all edges of enhancement cell even using the proposed CLR. We visualize the architecture weights with respect to each edge of convolution and enhancement cells in Fig. 7. Obviously, the proposed CLR can not make the *skip connection* (i.e. the blue line) out of predominance, especially for the enhancement cell. Moreover, full *skip connection*-consisted enhancement cell dose not work for broad scalable architecture. As described in DARTS+ [7], the first cell employs fresh images as input and the input of last one is mixed with lots of noises, so that the enhancement cell suffers from the collapse issue worse than the convolutional one.

### B. Confidence Factor Determination

In order to determine optimal  $\beta$  under **Criterion 1**, we set it from 1 to 4 for architecture search. The architecture weights  $\alpha$

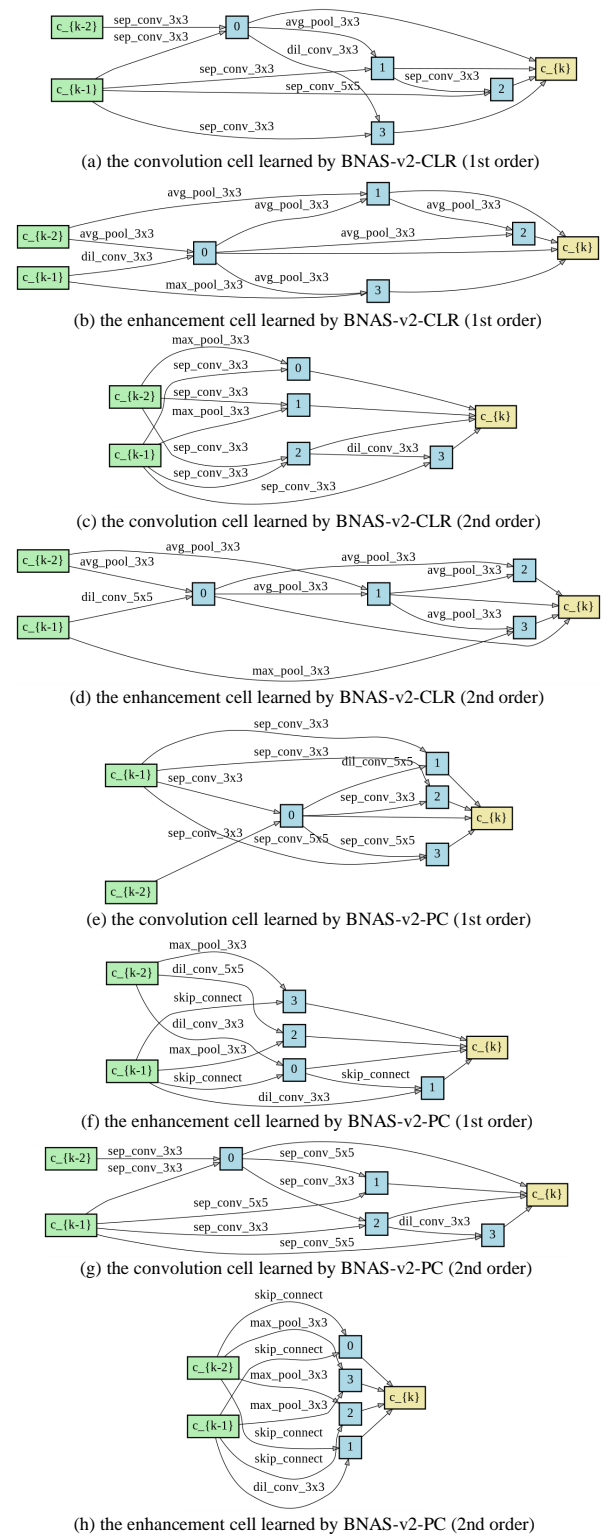


Fig. 9. The architectures learned by BNAS-v2 on CIFAR-10.

with respect to the shallowest edge (connecting the first input node  $x_{(0)}$  and the first intermediate node  $x_{(2)}$ ) is chosen as the index for confidence factor determination. We show the experimental results for BNAS-v2-CLR in Fig. 8.

For the first case of BNAS-v2-CLR,  $\alpha$  starts to be updated before 10-th epoch. For  $\beta = 3$  and  $\beta = 4$ , the starting

TABLE II  
COMPARISON OF THE PROPOSED BNAS-v2 AND OTHER STATE-OF-THE-ART NAS APPROACHES ON CIFAR-10.

Architecture	Error (%)	Params (M)	Search Cost (GPU days)	Search Method	Number of Cells	Topology
LEMONADE [30]	3.05	4.7	80	evolution	-	deep
DARTS (1st order) [4]	$3.00 \pm 0.14$	3.3	0.45 <sup>†</sup>	gradient-based	20	deep
DARTS (2nd order) [4]	$2.76 \pm 0.09$	3.3	1.50 <sup>†</sup>	gradient-based	20	deep
SNAS + mild constraint [6]	2.98	2.9	1.5	gradient-based	20	deep
SNAS + moderate constraint [6]	$2.85 \pm 0.02$	2.8	1.5	gradient-based	20	deep
SNAS + aggressive constraint [6]	$3.10 \pm 0.04$	<b>2.3</b>	1.5	gradient-based	20	deep
P-DARTS [5]	<b>2.50</b>	3.4	0.30	gradient-based	20	deep
PC-DARTS (1st order) [8]	$2.57 \pm 0.07$	3.6	0.10	gradient-based	20	deep
PC-DARTS (2nd order) [8]	-	-	OOM <sup>‡</sup>	gradient-based	-	-
ENAS [3]	2.89	4.6	0.45	RL	17	deep
BNAS [10]	2.97	4.7	0.20	RL	<b>5</b>	broad
BNAS-CCLE [10]	2.95	4.1	0.20	RL	<b>5</b>	broad
BNAS-CCE [10]	2.88	4.8	0.19	RL	8	broad
BNAS-v2-CLR (1st order) (ours)	$2.67 \pm 0.12$	3.3	0.09	gradient-based	8	broad
BNAS-v2-CLR (2nd order) (ours)	$2.80 \pm 0.09$	3.2	0.19	gradient-based	8	broad
BNAS-v2-PC (1st order) (ours)	$2.79 \pm 0.19$	3.7	<b>0.05</b>	gradient-based	8	broad
BNAS-v2-PC (2nd order) (ours)	$2.77 \pm 0.09$	3.5	0.09	gradient-based	8	broad

<sup>†</sup> Obtained by DARTS using the code publicly released by the authors at <https://github.com/quark0/darts> on a single NVIDIA GTX 1080Ti GPU.

<sup>‡</sup> Obtained by PC-DARTS using the code publicly released by the authors at <https://github.com/yuhuixu1993/PC-DARTS> with default setting for 1st order approximation of batch size 256 on a single NVIDIA GTX 1080Ti GPU.

epochs of weights update are both larger than 20. The case of  $\beta = 2$  satisfies **Criterion 1**, i.e. starting to train architecture weights from about 15-th epoch. Consequently,  $\beta$  is set to 2 for the following experiments with regard to BNAS-v2-CLR. Furthermore, we find an interesting phenomenon from Fig. 8, that the *none* operation (i.e. red line) always achieves the largest weight when using various confidence factors. The above phenomenon indicates that the proposed CLR does only modify the tendency of weight-equipped operations in later training epochs, rather than imposing small architecture weight on weight-free operations in early training phase.

### C. Experiments on CIFAR-10

1) *Experimental Settings*: In the architecture search phases of BNAS-v2-CLR and BNAS-v2-PC, there are many identical experimental details as below. The over-parameterized BCNN consists of 3 cells (2 broad cells and 1 enhancement cell), where each one contains 2 input nodes, 4 intermediate nodes and 1 output node. We set the number of initial input channels to 16 and train the over-parameterized BCNN for 50 epochs. The split portion of proxy dataset is set to 0.5, i.e. two subsets, each one with 25K training data of CIFAR-10, that are used for training the over-parameterized BCNN and architecture weights, respectively. The SGD optimizer [34] is employed to optimize the network weights  $w$ , with dynamic learning rate (annealed down to zero following a cosine schedule without restart), momentum 0.9, weight decay  $3 \times 10^{-4}$ . For architecture weights, we use zero initialization to generate  $\alpha$  for both convolution and enhancement cells. Moreover, we utilize Adam [35] with momentum (0.5, 0.999) and weight decay  $10^{-3}$ , as the optimizer to update  $\alpha$ . We run four repeated experiments of architecture search for BNAS-v2-CLR and

BNAS-v2-PC, and choose the best performing architecture as the optimal one. There are also some differences between the experimental settings of BNAS-v2-CLR and BNAS-v2-PC as follows. On one hand, the learning rate of architecture weights  $\eta_\alpha$  is set to  $3 \times 10^{-4}$  in BNAS-v2-CLR. Moreover, we employ CLR with  $\beta = 2$  to mitigate the performance collapse issue of BNAS-v2. Beyond that, we set the batch size and learning rate to 256 and 0.1 for architecture search, respectively. On the other hand,  $\eta_\alpha$  used for BNAS-v2-PC is set to  $6 \times 10^{-4}$ . The strategy of partial channel connections contributes BNAS-v2-PC to discover novel architecture with batch size 512 and learning rate 0.2, due to the contribution of memory efficiency.

For the architecture evaluation stage, BNAS-v2-CLR and BNAS-v2-PC use identical experimental settings as follows. BCNN is constructed by stacking 8 cells (2 deep cells and 1 broad cell in each convolution block, and 2 enhancement cells). We tune the number of initial input channels to fit the parameters following a mobile setting between 3~4M. Furthermore, BCNN is trained for 2000 epochs using SGD optimizer with batch size 128, initial learning rate 0.025 (the decayed way following the search phase), momentum 0.9, weight decay  $3 \times 10^{-4}$ . Moreover, cutout with 16 length [36] and drop path with a probability of 0.3 are adopted as previous NAS works. The experimental results (*mean  $\pm$  std*) are obtained by three repeated experiments.

2) *Results and Analysis*: We visualize the best performing architectures learned by BNAS-v2-CLR and BNAS-v2-PC in Fig. 9. Furthermore, TABLE II summarizes the comparison of the proposed BNAS-v2 with other state-of-the-art NAS approaches.

The proposed BNAS-v2 takes full advantages of BCNN, so that great efficiency improvement can be obtained as shown

TABLE III  
COMPARISON OF THE PROPOSED BNAS-v2 AND OTHER STATE-OF-THE-ART NAS APPROACHES ON IMAGENET

Architecture	Test Err. (%)		Params (M)	Search Cost (GPU days)	Mult-Adds (M)	Topology
	top-1	top-5				
Inception-v1 [14]	30.2	10.1	6.6	-	1448	deep
MobileNet [37]	29.4	10.5	4.2	-	569	deep
ShuffleNet [38]	26.4	10.2	~5	-	524	deep
AmoebaNet-A [9]	25.5	8.0	5.1	3150	555	deep
AmoebaNet-B [9]	26.0	8.5	5.3	3150	555	deep
AmoebaNet-C [9]	24.3	7.6	6.4	3150	570	deep
NASNet-A [2]	26.0	8.4	5.3	1800	564	deep
NASNet-B [2]	27.2	8.7	5.3	1800	488	deep
NASNet-C [2]	27.5	9.0	4.9	1800	558	deep
PNAS [39]	25.8	8.1	5.1	225	588	deep
DARTS (2nd order) [4]	26.7	8.7	4.7	1.50	574	deep
ProxylessNAS (GPU) [40] †	24.9	7.5	7.1	8.30	465	deep
SNAS (mild) [6]	27.3	9.2	4.3	1.50	522	deep
P-DARTS (CIFAR-10) [5]	24.4	7.4	4.9	0.30	557	deep
P-DARTS (CIFAR-100)[5]	24.7	7.5	5.1	0.30	577	deep
PC-DARTS (CIFAR-10)[8]	25.1	7.8	5.3	0.10	586	deep
PC-DARTS (ImageNet) [8]†	<b>24.2</b>	<b>7.3</b>	5.3	3.80	597	deep
BNAS [10]	25.7	7.8	3.9	0.20	-	broad
BNAS-v2-CLR-C2 (1st order) (ours)	27.3	9.0	4.4	<b>0.09</b>	<b>441</b>	broad
BNAS-v2-CLR-C5 (1st order) (ours)	27.2	9.0	<b>3.7</b>	<b>0.09</b>	938	broad
BNAS-v2-PC-C2 (2nd order) (CIFAR-10) (ours)	27.2	8.8	4.6	<b>0.09</b>	475	broad
BNAS-v2-PC-C2 (ImageNet) (ours)†	27.0	10.5	4.6	<b>0.19</b> ‡	576	broad

† Those architectures are discovered on ImageNet directly.

‡ State-of-the-art efficiency for proxyless architecture search on ImageNet.

in TABLE II. Moreover, BNAS-v2 also achieves satisfactory accuracy. Particularly, BNAS-v2-PC (1st order) achieves 3.8x faster efficiency (state-of-the-art efficiency of 0.05 GPU days) and higher accuracy (i.e.  $2.79 \pm 0.19\%$  test error) than BNAS-CCE [10] whose broad scalable architecture is identical with BNAS-v2. Compared with continuous relaxation-based DARTS [4], the efficiency of BNAS-v2-CLR is 5x (0.09 GPU days) and 7.9x (0.19 GPU days) faster when using 1st and 2nd approximation orders, respectively. Beyond that, BNAS-v2-CLR also delivers higher accuracy due to the contribution of the proposed CLR. Compared with partial-connected PC-DARTS [8], BNAS-v2-PC achieves state-of-the-art efficiency, 2x less computational cost (about 70 minutes) by using 1st order approximation. Beyond that, BNAS-v2-PC obtains competitive  $2.79 \pm 0.19$  test error with 3.7M parameters. In particular, PC-DARTS suffers from the Out of Memory (OOM) issue when using 2nd order approximation with batch size 256 on a single NVIDIA GTX 1080Ti GPU (refer to TABLE II). The reason is that there are no memory to construct an extra model for architecture search with 2nd order approximation in PC-DARTS (using about 12G memory with batch size 256). However, BNAS-v2-PC does not suffer from the above OOM issue, due to enough memory is available for new model construction even though using batch size 512 for architecture search. Beyond that, due to the contribution of BCNN, all learned architectures achieve competitive even better performance just using 8 cells, instead of more than 17

cells. This characteristic implies that the architecture learned by BNAS-v2 excels in obtaining faster training and inference speed than those NAS approaches using deep scalable architecture for real-world applications, e.g. mobile devices.

#### D. Results on ImageNet

In this section, we do not only verify the transferability of the best performing architectures learned by BNAS-v2-CLR (1st order) and BNAS-v2-PC (2nd order), but also directly implement architecture search on ImageNet using BNAS-v2-PC.

##### 1) Experimental Settings for Transferability Verification:

In previous works using deep scalable architecture, the learned architecture is transferred to ImageNet by the following way. Three  $3 \times 3$  convolutions with stride 2 are treat as the stem layers to reduce the resolution of input images from  $224 \times 224$  to  $28 \times 28$ . Subsequently, the architecture learned on CIFAR-10 can be employed for image classification on ImageNet. Similarly, we leverage this way for the proposed approach named as BNAS-v2-C2 (e.g. BNAS-v2-CLR-C2, BNAS-v2-PC-C2 (CIFAR-10)), i.e. using 2 convolution blocks to construct the ImageNet classifier. Beyond that, another way for BCNN construction can be adopted. As described in BNAS [10], the number of convolution block is determined by the input size of the first convolution block, which is similar to the number of reduction cell in deep scalable architecture. Consequently, we also employ 5 convolution



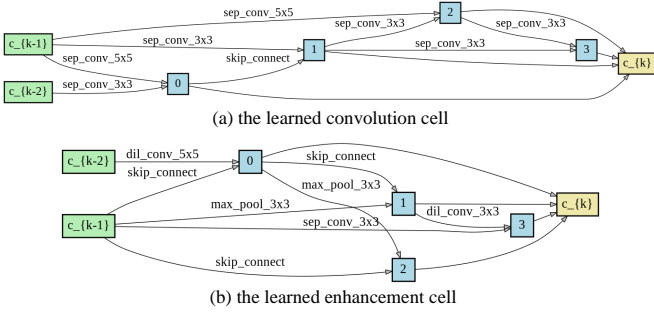


Fig. 10. The architecture learned by BNAS-v2-PC on ImageNet.

blocks to construct the ImageNet classifier named BNAS-v2-C5 (e.g. BNAS-v2-CLR-C5), for achieving possible better performance with full-scale representations. For BNAS-v2-C2, we set both the number of deep cell in each convolution block and enhancement cell to 2. For BNAS-v2-C5, there are 11 cells (1 deep cell and 1 broad cell in each convolution block, and 1 enhancement cell in each enhancement block) in the network. In the architecture evaluation phase of BNAS-v2-C5 on ImageNet, we train the architecture for 150 epochs with batch size 768 using 8 NVIDIA Tesla V100 GPUs. We also choose SGD as the optimizer with initial learning rate 0.1 (decayed by a factor of 0.1 at 80-th, 120-th and 140-th epoch), momentum 0.9 and weight decay  $3 \times 10^{-5}$ . Moreover, the initial input channels of BNAS-v2-C5 are set to 6, the label smoothing is set to 0.1, and the gradient clip bound is set to 5.0. Due to the topology difference, BNAS-v2-C2 can set larger batch size and learning rate than BNAS-v2-C5 for training on ImageNet. Consequently, we leverage various hyper-parameters from BNAS-v2-C5 in terms of batch size, the initial value and decayed way of learning rate for BNAS-v2-C2 as follows. We train BNAS-v2-C2 for 250 epochs with batch size 1024 using 2 NVIDIA Tesla V100 GPUs. Similarly, we also choose the SGD optimizer with initial learning rate 0.5 whose decayed way is identical with PC-DARTS [8] used for ImageNet. Moreover, the initial input channels of BNAS-v2-CLR-C2 and BNAS-v2-PC-C2 (CIFAR-10) are set to 48 and 50, respectively.

2) *Experimental Settings for Proxyless Architecture Search:* Two subsets contained 10% and 2.5% of 1.3 millions images, are randomly sampled from each category of training data of ImageNet for over-parameterized BCNN and architecture weights training, respectively. Similar to the search phase of PC-DARTS [8] on ImageNet, we treat three  $3 \times 3$  convolutions with stride 2 as the stem layers to reduce the resolution of input images from  $224 \times 224$  to  $28 \times 28$ . Subsequently, the over-parameterized BCNN used on CIFAR-10 can be employed for proxyless architecture search on ImageNet. Here, we use a single Tesla V100 GPU to discover architecture, and set the batch size and learning rate to 512 and 0.2, respectively. Other hyper-parameters are similar to BNAS-v2-PC used for architecture search on CIFAR-10. For the architecture directly learned on imageNet, we construct the classifier with 2 convolution blocks by stacking 10 cells (3 deep cells in each convolution block, and a single enhancement block).

3) *Results and Analysis:* We visualize the convolution and enhancement cells learned by BNAS-v2-PC on ImageNet in Fig. 10, and summarize the comparison of BNAS-v2-PC (ImageNet) and other NAS approaches on ImageNet in TABLE III.

On one hand, both two BNAS-v2-CLR-based classifiers achieve competitive performance in terms of test error. Moreover, BNAS-v2-CLR-C5 achieves better accuracy with less parameters than BNAS-v2-CLR-C2. The above result implies that the strategy of multi-scale feature fusion contributes to the performance improvement of broad scalable architecture. Furthermore, the index of Mult-Adds of BNAS-v2-CLR-C2 is state-of-the-art. However, BNAS-v2-CLR-C5 has the largest index of Mult-Adds in TABLE III which dose not satisfy the mobile setting (i.e. smaller than 600M), even its index of parameters is just 3.7M. Here, the first three convolution blocks where the size of input is too large, lead to the above catastrophic phenomenon.

On the other hand, BNAS-v2-PC also delivers state-of-the-art search efficiency for proxyless architecture search on ImageNet. The entire search process spends around 4.6 hours (about 20x faster than state-of-the-art PC-DARTS) on a single NVIDIA Tesla V100 GPU. In addition, the indices of parameters and Mult-Adds of both two architectures learned by BNAS-v2-PC are better than vanilla PC-DARTS, especially for the later one. Beyond that, all architectures learned by BNAS-v2 achieve competitive accuracy just using few parameters, that verify the contribution of the multi-scale feature fusion of BCNN again. Moreover, the architecture directly learned on ImageNet outperforms the one learned on proxy data in terms of the top-1 accuracy. This indicates that the proposed BNAS-v2-PC is effective for proxyless architecture search on ImageNet.

Admittedly, there exists a performance gap for ImageNet classification between BNAS-v2 and PC-DARTS, i.e. broad and deep scalable architectures. Due to the restriction of computational resources, we can not determine a list of appropriate hyper-parameters for the learned broad architectures, e.g. the number of deep and enhancement cells. Beyond that, we argue that the number of convolution blocks plays an important role for broad deep scalable architecture in ImageNet classification task. This is similar to the backbone design of YOLOv3 [41], which obtains better detection performance using multi-scale prediction, i.e. feature maps with the sizes of  $32 \times 32$ ,  $16 \times 16$ , and  $8 \times 8$ , than previous versions of YOLO. As a result, the optimal list of hyper-parameters including the number of convolution blocks, needs to be determined further through intensive experiments for large scale image classification. We believe that the above performance gap can be bridged with an optimal list of appropriate hyper-parameters in the future.

#### E. Effectiveness of Confident Learning Rate

In this part, we implement two groups of ablation experiments with respect to BNAS-D and DARTS, to examine the effectiveness of the proposed CLR for performance collapse alleviation. To some extent, the number of convolutions in two types of cells,  $\theta$ , is basically proportional to the accuracy of

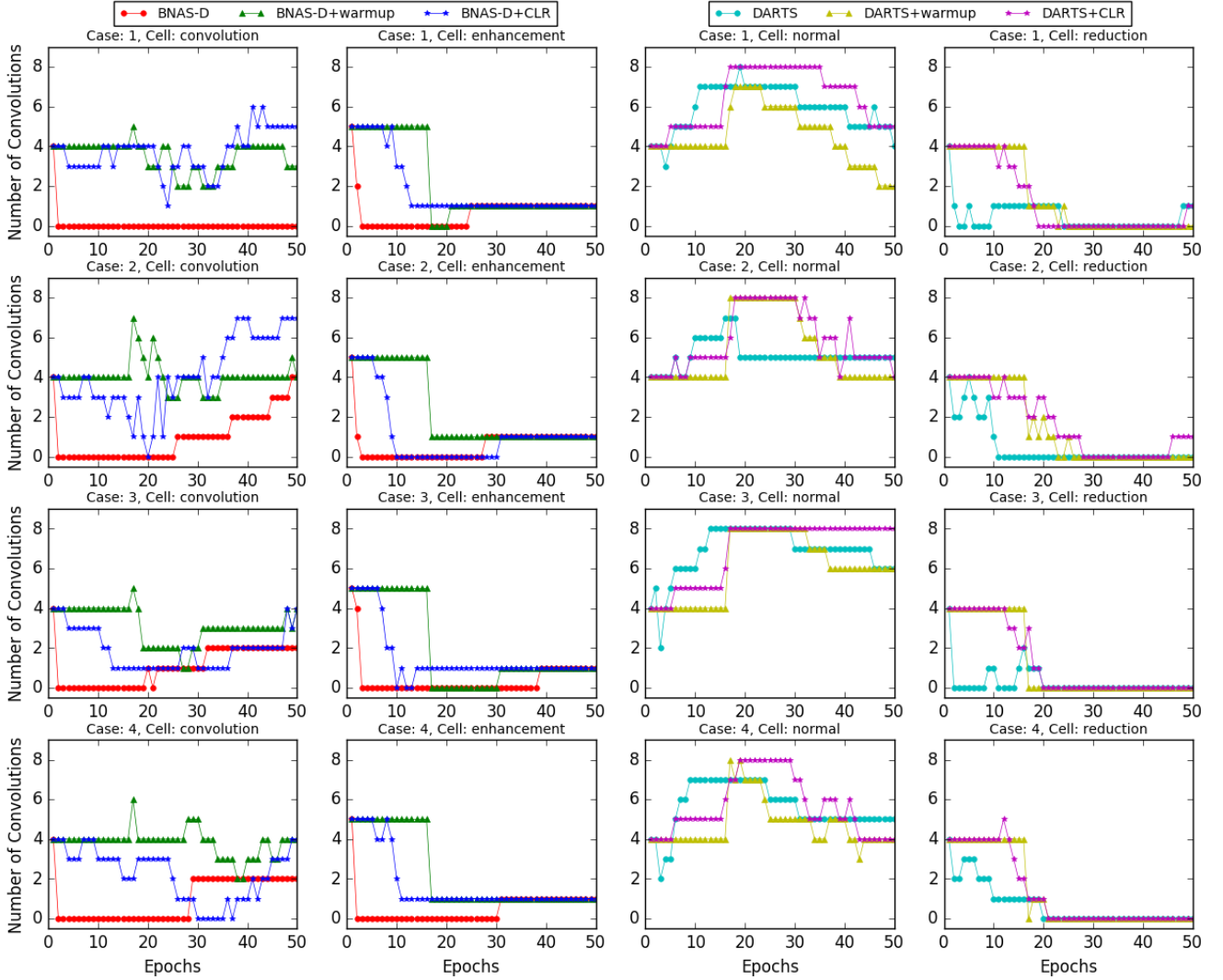


Fig. 11. The number of convolutions of entire search process in two cells learned by BNAS-D/DARTS, BNAS-D/DARTS with warmup and BNAS-D/DARTS with CLR under four repeated implementations where the confidence factor are set to 2 and 4 for BNAS-D and DARTS, respectively. Moreover, BNAS-D+CLR is identical with BNAS-v2-CLR. We use the sum of the number of convolution operations with regard to two cells as the index for performance evaluation. Best viewed in color.

model [42], so that we employ  $\theta$  as the index to examine the effectiveness of CLR for both BNAS-D and vanilla DARTS. Furthermore, we choose warmup strategy as the comparative method to further verify the effectiveness of CLR. We repeat running six method, vanilla BNAS-D/DARTS, BNAS-D/DARTS with warmup, and BNAS-D/DARTS with CLR, for four times, and show the number of convolutions of entire search process in Fig. 11.

For vanilla performance-collapse-suffered BNAS-D, the mean value of  $\theta$  is about 3 which tends to deliver poor performance. Moreover, we train the architecture of case 2 (most convolution operations in the learned architecture over four cases) learned by vanilla BNAS-D for 600 epochs. The architecture achieves 3.26% test error with 3.6M parameters under default hyper-parameters of BNAS-v2-CLR. The warmup strategy contributes to the performance collapse issue mitigation of BNAS-D in terms of  $\theta$ , where the mean value of  $\theta$  is about 4.5. For the proposed CLR,  $\theta$  of four repeated implementations are 6, 8, 5, 5 (i.e. the sum of convolutions

in both convolution and enhancement cells), respectively. Obviously, there are more convolutions in the learned cells by BNAS-D with CLR than warmup. Moreover, we also train the architecture of case 1 learned by BNAS-D using CLR for 600 epochs. The architecture achieves 2.90% test error with 3.4M parameters under the above settings for architecture evaluation.

From the overall perspective,  $\theta$  for BNAS-D with CLR (i.e. BNAS-v2-CLR) decreases firstly, and then increases to a high value. In the decreasing phase of  $\theta$ , those weight-free operations are prone to be equipped with larger weights than the weight-equipped one, although the confident learning rate is small enough. The reason of above situation is that the outputs of weight-free operations are more consistent with its input, which is preferred by gradient-based search algorithm [8]. With the convergence of over-parameterized BCNN, the increasing phase of  $\theta$  begins. Those well-optimized weight-equipped operations contribute to the improvement of validation accuracy, so that the search strategy starts to prefer them.

Different from BNAS-D, we set the value of confidence factor  $\beta$  to 4 rather than 2. Through extensive experiments, we draw a conclusion that  *$\beta$  those deep scalable architectures should be equipped with larger value of  $\beta$  than the broad one, for training the over-parameterized model well.* For vanilla DARTS, the mean value of  $\theta$  is about 5, and only the first implementation learns to utilize a convolutional operation in reduction cell. Here, a convolution in reduction cell tends to achieve satisfactory performance with larger probability than those cells consisted of all weight-free operations. Beyond that, DARTS with warmup delivers equal or worse performance than vanilla DARTS in terms of the number of convolutional operations. Moreover, it can not learn to employ convolutional operation in reduction cell for possible improvement. DARTS with CLR learns 6, 5, 8, 4 convolutions under four repeated implementations, whose mean value is about 6 (1 larger than vanilla DARTS). Importantly, the proposed CLR excels in discovering the reduction cell of DARTS with convolutional operation.

## V. CONCLUSIONS

BNAS can not take full advantages of BCNN for architecture search, due to the influence of unfair training issue. In order to improve the efficiency of BNAS further, we propose BNAS-v2. Particularly, we employ the strategy of continuous relaxation to mitigate the unfair training issue in BNAS. However, a consequent issue of continuous relaxation named performance collapse arises. For this, we provide two solutions in BNAS-v2, i.e. BNAS-v2-CLR and BNAS-v2-PC. On one hand, we propose Confident Learning Rate (CLR) in BNAS-v2-CLR, that considers the confidence of gradient for architecture weights update increasing with the training time of over-parameterized BCNN, to mitigate the issue of performance collapse. On the other hand, for BNAS-v2-PC, we introduce the combination of partial channel connections and edge normalization that can not only alleviate the performance issue, but also make BNAS-v2-PC more memory-efficient than BNAS-v2-CLR.

The proposed BNAS-v2 delivers state-of-the-art efficiency on both CIFAR-10 and ImageNet. Particularly, BNAS-v2-PC achieves 3.8x faster efficiency (state-of-the-art efficiency of 0.05 GPU days) and higher accuracy (i.e.  $2.79 \pm 0.19\%$  test error) on CIFAR-10 than BNAS-CCE whose broad scalable architecture is identical with BNAS-v2. Furthermore, BNAS-v2 also can realize the proxyless architecture search on ImageNet with state-of-the-art efficiency of 0.19 GPU days. Beyond that, the proposed CLR contributes both BNAS-v2 and DARTS to learn more convolutions in two types of cells for performance improvement. However, BNAS-v2 dose not always improve the efficiency without performance drop, especially for large scale image classification task. We will utilize knowledge distillation [43] to solve this issue in the future.

## REFERENCES

- [1] B. Zoph and Q. V. Le, "Neural architecture search with reinforcement learning," in *International Conference on Learning Representations (ICLR)*, 2017.
- [2] B. Zoph, V. Vasudevan, J. Shlens, and Q. V. Le, "Learning transferable architectures for scalable image recognition," in *Proceedings of the IEEE Conference on Computer Vision and Pattern Recognition (CVPR)*, 2018, pp. 8697–8710.
- [3] H. Pham, M. Guan, B. Zoph, Q. Le, and J. Dean, "Efficient neural architecture search via parameters sharing," in *International Conference on Machine Learning (ICLR)*, 2018, pp. 4095–4104.
- [4] H. Liu, K. Simonyan, Y. Yang *et al.*, "Darts: Differentiable architecture search," in *International Conference on Learning Representations (ICLR)*, 2018.
- [5] X. Chen, L. Xie, J. Wu, and Q. Tian, "Progressive differentiable architecture search: Bridging the depth gap between search and evaluation," in *Proceedings of the IEEE International Conference on Computer Vision (ECCV)*, 2019, pp. 1294–1303.
- [6] S. Xie, H. Zheng, C. Liu, and L. Lin, "Snas: stochastic neural architecture search," in *International Conference on Learning Representations (ICLR)*, 2018.
- [7] H. Liang, S. Zhang, J. Sun, X. He, W. Huang, K. Zhuang, and Z. Li, "Darts+: Improved differentiable architecture search with early stopping," *arXiv preprint arXiv:1909.06035*, 2019.
- [8] Y. Xu, L. Xie, X. Zhang, X. Chen, G.-J. Qi, Q. Tian, and H. Xiong, "PC-DARTS: Partial channel connections for memory-efficient architecture search," in *International Conference on Learning Representations (ICLR)*, 2019.
- [9] E. Real, A. Aggarwal, Y. Huang, and Q. V. Le, "Regularized evolution for image classifier architecture search," in *Proceedings of the AAAI Conference on Artificial Intelligence (AAAI)*, vol. 33, 2019, pp. 4780–4789.
- [10] Z. Ding, Y. Chen, N. Li, D. Zhao, Z. Sun, and C. Chen, "BNAS: An efficient neural architecture search approach using broad scalable architecture," *arXiv preprint arXiv:2001.06679v2*, 2020.
- [11] R. J. Williams, "Simple statistical gradient-following algorithms for connectionist reinforcement learning," *Machine Learning*, vol. 8, no. 3-4, pp. 229–256, 1992.
- [12] X. Chu, B. Zhang, R. Xu, and J. Li, "Fairnas: Rethinking evaluation fairness of weight sharing neural architecture search," *arXiv preprint arXiv:1907.01845*, 2019.
- [13] K. He, X. Zhang, S. Ren, and J. Sun, "Deep residual learning for image recognition," in *Proceedings of the IEEE Conference on Computer Vision and Pattern Recognition (CVPR)*, 2016, pp. 770–778.
- [14] C. Szegedy, W. Liu, Y. Jia, P. Sermanet, S. Reed, D. Anguelov, D. Erhan, V. Vanhoucke, and A. Rabinovich, "Going deeper with convolutions," in *Proceedings of the IEEE Conference on Computer Vision and Pattern Recognition (CVPR)*, 2015, pp. 1–9.
- [15] D. Zhao, Y. Chen, L. Lv *et al.*, "Deep reinforcement learning with visual attention for vehicle classification," *IEEE Transactions on Cognitive and Developmental Systems*, vol. 9, no. 4, pp. 356–367, 2017.
- [16] Y. Chen, D. Zhao, L. Lv, and Q. Zhang, "Multi-task learning for dangerous object detection in autonomous driving," *Information Sciences*, vol. 432, pp. 559–571,

- 2018.
- [17] S. Wen, W. Liu, Y. Yang, P. Zhou, Z. Guo, Z. Yan, Y. Chen, and T. Huang, "Multilabel image classification via feature/label co-projection," *IEEE Transactions on Systems, Man, and Cybernetics: Systems*, 2020.
  - [18] X. Wang, A. Bao, E. Lv, and Y. Cheng, "Multiscale multipath ensemble convolutional neural network," *IEEE Transactions on Systems, Man, and Cybernetics: Systems*, 2020.
  - [19] G. Chen, H. Wang, K. Chen, Z. Li, Z. Song, Y. Liu, W. Chen, and A. Knoll, "A survey of the four pillars for small object detection: Multiscale representation, contextual information, super-resolution, and region proposal," *IEEE Transactions on Systems, Man, and Cybernetics: Systems*, 2020.
  - [20] H. Kuang, L. Chen, L. L. H. Chan, R. C. Cheung, and H. Yan, "Feature selection based on tensor decomposition and object proposal for night-time multiclass vehicle detection," *IEEE Transactions on Systems, Man, and Cybernetics: Systems*, vol. 49, no. 1, pp. 71–80, 2019.
  - [21] A. Vaswani, N. Shazeer, N. Parmar, J. Uszkoreit, L. Jones, A. N. Gomez, Ł. Kaiser, and I. Polosukhin, "Attention is all you need," in *Advances in Neural Information Processing Systems (NIPS)*, 2017, pp. 5998–6008.
  - [22] X. Tao, D. Zhang, Z. Wang, X. Liu, H. Zhang, and D. Xu, "Detection of power line insulator defects using aerial images analyzed with convolutional neural networks," *IEEE Transactions on Systems, Man, and Cybernetics: Systems*, vol. 50, no. 4, pp. 1486–1498, 2020.
  - [23] H. Li, Q. Zhang, D. Zhao *et al.*, "Deep reinforcement learning-based automatic exploration for navigation in unknown environment," *IEEE Transactions on Neural Networks and Learning Systems*, vol. 31, no. 6, pp. 2064–2076, 2020.
  - [24] A. Kamel, B. Sheng, P. Yang, P. Li, R. Shen, and D. D. Feng, "Deep convolutional neural networks for human action recognition using depth maps and postures," *IEEE Transactions on Systems, Man, and Cybernetics: Systems*, vol. 49, no. 9, pp. 1806–1819, 2019.
  - [25] K. Shao, Y. Zhu, D. Zhao *et al.*, "Starcraft micromanagement with reinforcement learning and curriculum transfer learning," *IEEE Transactions on Emerging Topics in Computational Intelligence*, vol. 3, no. 1, pp. 73–84, 2019.
  - [26] Y. Chen, R. Gao, F. Liu, and D. Zhao, "Modulenet: Knowledge-inherited neural architecture search," *arXiv preprint arXiv:2004.05020*, 2020.
  - [27] Y. Sun, B. Xue, M. Zhang, G. G. Yen, and J. Lv, "Automatically designing cnn architectures using the genetic algorithm for image classification," *IEEE Transactions on Cybernetics*, vol. 50, no. 9, pp. 3840–3854, 2020.
  - [28] C. Liu, L.-C. Chen, F. Schroff, H. Adam, W. Hua, A. L. Yuille, and L. Fei-Fei, "Auto-deeplab: Hierarchical neural architecture search for semantic image segmentation," in *Proceedings of the IEEE conference on Computer Vision and Pattern Recognition (CVPR)*, 2019, pp. 82–92.
  - [29] H. Zhu and Y. Jin, "Multi-objective evolutionary federated learning," *IEEE transactions on neural networks and learning systems*, vol. 31, no. 4, pp. 1310–1322, 2020.
  - [30] T. Elsken, J. H. Metzen, F. Hutter *et al.*, "Efficient multi-objective neural architecture search via lamarckian evolution," in *International Conference on Learning Representations (ICLR)*, 2018.
  - [31] C. P. Chen, Z. Liu, S. Feng *et al.*, "Universal approximation capability of broad learning system and its structural variations," *IEEE Transactions on Neural Networks and Learning Systems*, vol. 30, no. 4, pp. 1191–1204, 2018.
  - [32] A. Krizhevsky and G. Hinton, "Learning multiple layers of features from tiny images," 2009.
  - [33] O. Russakovsky, J. Deng, H. Su, J. Krause, S. Satheesh, S. Ma, Z. Huang, A. Karpathy, A. Khosla, M. Bernstein *et al.*, "Imagenet large scale visual recognition challenge," *International Journal of Computer Vision*, vol. 115, no. 3, pp. 211–252, 2015.
  - [34] I. Loshchilov and F. Hutter, "SGDR: Stochastic gradient descent with warm restarts," in *International Conference on Machine Learning (ICML)*, 2017.
  - [35] D. Kingma and L. Ba, "Adam: A method for stochastic optimization," in *International Conference on Learning Representations (ICLR)*, 2015.
  - [36] T. Devries and G. W. Taylor, "Improved regularization of convolutional neural networks with cutout," *arXiv preprint arXiv:1708.04552*, 2017.
  - [37] A. G. Howard, M. Zhu, B. Chen, D. Kalenichenko, W. Wang, T. Weyand, M. Andreetto, and H. Adam, "Mobilenets: Efficient convolutional neural networks for mobile vision applications," *arXiv preprint arXiv:1704.04861*, 2017.
  - [38] X. Zhang, X. Zhou, M. Lin, and J. Sun, "Shufflenet: An extremely efficient convolutional neural network for mobile devices," in *Proceedings of the IEEE Conference on Computer Vision and Pattern Recognition (CVPR)*, 2018, pp. 6848–6856.
  - [39] C. Liu, B. Zoph, M. Neumann, J. Shlens, W. Hua, L. Li, L. FeiFei, A. Yuille, J. Huang, and K. Murphy, "Progressive neural architecture search," in *Proceedings of the European Conference on Computer Vision (ECCV)*, 2018, pp. 19–34.
  - [40] H. Cai, L. Zhu, S. Han *et al.*, "Proxylessnas: Direct neural architecture search on target task and hardware," in *International Conference on Learning Representations (ICLR)*, 2018.
  - [41] J. Redmon and A. Farhadi, "Yolov3: An incremental improvement," *arXiv preprint arXiv:1804.02767*, 2018.
  - [42] M. Guo, Y. Yang, R. Xu, Z. Liu, and D. Lin, "When nas meets robustness: In search of robust architectures against adversarial attacks," in *Proceedings of the IEEE Conference on Computer Vision and Pattern Recognition (CVPR)*, 2020, pp. 631–640.
  - [43] B. Heo, M. Lee, S. Yun, and J. Y. Choi, "Knowledge distillation with adversarial samples supporting decision boundary," in *Proceedings of the AAAI Conference on Artificial Intelligence (AAAI)*, vol. 33, 2019, pp. 3779–3787.